General Disclaimer

One or more of the Following Statements may affect this Document

- This document has been reproduced from the best copy furnished by the organizational source. It is being released in the interest of making available as much information as possible.

- This document may contain data, which exceeds the sheet parameters. It was furnished in this condition by the organizational source and is the best copy available.

- This document may contain tone-on-tone or color graphs, charts and/or pictures, which have been reproduced in black and white.

- This document is paginated as submitted by the original source.

- Portions of this document are not fully legible due to the historical nature of some of the material. However, it is the best reproduction available from the original submission.

Produced by the NASA Center for Aerospace Information (CASI)

NASA TECHNICAL
MEMORANDUM

NASA TM X-62,465

NASA TM X-62,465

(NASA-TM-X-62465) A HOT-WIRE SURFACE GAGE FOR SKIN FRICTION AND SEPARATION DETECTION MEASUREMENTS (NASA) 12 p HC $3.25 CSCL 14B

N75-29384

Unclas
G3/35 32360

A HOT-WIRE SURFACE GAGE FOR SKIN FRICTION AND SEPARATION DETECTION MEASUREMENTS

Morris W. Rubesin, Arthur F. Okuno, George G. Mateer, and Aviel Brosh

Ames Research Center
Moffett Field, California 94035

July 1975

1. Report No.	2. Government Accession No.	3. Recipient's Catalog No.
TM X-62,465		

4. Title and Subtitle	5. Report Date
A HOT-WIRE SURFACE GAGE FOR SKIN FRICTION AND SEPARATION DETECTION MEASUREMENTS	6. Performing Organization Code

7. Author(s)	8. Performing Organization Report No.
Morris W. Rubesin, Arthur F. Okuno, George G. Mateer, and Aviel Brosh	A-6159
9. Performing Organization Name and Address	10. Work Unit No. 505-06-13
Ames Research Center, NASA Moffett Field, Calif. 94035	11. Contract or Grant No.
12. Sponsoring Agency Name and Address	13. Type of Report and Period Covered Technical Memorandum
National Aeronautics and Space Administration Washington, D. C. 20546	14. Sponsoring Agency Code

15. Supplementary Notes

16. Abstract

A heated-element, skin-friction gage employing a very low thermal conductivity support is described. It is shown that the effective dimension of the gage in the stream direction is only 0.06 mm, including the effects of heat conduction in the supporting material. Because of its small size, the calibration of the gage is independent of the kind of boundary-layer flow - whether laminar or turbulent - and is insensitive to pressure gradients. Further, construction tolerances can be maintained so that a single universal calibration can be applied. Finally, multiple gages, sufficiently closely spaced so as to interfere with each other, are shown to provide accurate determinations of the locations of the points of boundary-layer separation and reattachment.

17. Key Words (Suggested by Author(s))	18. Distribution Statement
Fluid mechanics	Unclassified - Unlimited STAR Category 34

19. Security Classif. (of this report)	20. Security Classif. (of this page)	21. No. of Pages	22. Price*
Unclassified	Unclassified	12	$3.25

*For sale by the National Technical Information Service, Springfield, Virginia 22151

A HOT-WIRE SURFACE GAGE FOR SKIN FRICTION AND SEPARATION DETECTION MEASUREMENTS

Morris W. Rubesin,* Arthur F. Okuno,† George C. Mateer,‡ and Ariel Brosh††

Ames Research Center, NASA, Moffett Field, Calif. 94035

Abstract. A heated-element, skin-friction gage employing a very low thermal conductivity support is described. It is shown that the effective dimension of the gage in the stream direction is only 0.06 mm, including the effects of heat conduction in the supporting material. Because of its small size, the calibration of the gage is independent of the kind of boundary-layer flow - whether laminar or turbulent - and is insensitive to pressure gradients. Further, construction tolerances can be maintained so that a single universal calibration can be applied. Finally, multiple gages, sufficiently closely spaced so as to interfere with each other, are shown to provide accurate determinations of the locations of the points of boundary-layer separation and reattachment.

SYMBOLS

c_f	local skin-friction coefficient, $\dfrac{\tau_w}{(1/2)\rho_e u_e^2}$, dimensionless
D	diameter of cylinder, m
h	amplitude of surface waviness, mm
i	current, A
M	Mach number, dimensionless
Nu	Nusselt number, dimensionless
Pr	Prandtl number of fluid, dimensionless
p	static pressure, N/m^2
R	resistance of heater element, Ω
Re	Reynolds number, dimensionless
S_ℓ	length of separated region, m
u	velocity of fluid, m/s
W	width of heated element, perpendicular to streamwise direction, m
ΔT	temperature rise of heated element above upstream surface temperature, °C
Δx	length of heated element in streamwise direction, m
δ_u	boundary-layer thickness upstream of disturbance, m
θ	angle from stagnation point, deg
μ	fluid viscosity, Ns/m^2
ρ	fluid density, kg/m^3
τ_w	surface shear or skin-friction stress, N/m^2

Subscripts

D	based on diameter
e	at boundary-layer edge
eff	effective, refers to length of heater element
FP	corresponding to a flat plate
t	total condition in a flow field
w	wall condition
∞	free-stream condition

INTRODUCTION

Recent developments in computer technology and numerical techniques have advanced the field of computational fluid mechanics to such an extent that it can be projected that supplemental computations will permit major reductions in the amount of wind-tunnel testing required for future aircraft development (1). Problems in aeronautics that were intractable by mathematical analysis are currently being solved routinely through numerical computations. Involved in these computations are such features as three dimensions, complex configurations, large pressure gradients along and normal to body surfaces, and even extensive regions of separation where there are strong interactions between the viscous and inviscid portions of the flow.

The main thrust of the computations has been in laminar flow problems because the physics and governing mathematical descriptions of such flows are well understood. For turbulent flows, however, even the best of computers cannot be expected to resolve the turbulence to the scales of the smallest significant eddies where the basic equations, based on molecular processes, still apply. Approximations to the turbulence mechanisms, or "turbulence modeling" (2), must be introduced to permit low spatial resolution computations consistent with computer capabilities. Historically, turbulence models evolved from well-controlled fluid mechanical experiments, and the need for such experiments, extended to the complexities of the flow fields mentioned above, is as critical as ever. Moreover, as the turbulence models become more sophisticated, they require increasingly complex measurements in the experiments.

Improved turbulence models and continued progress in computational fluid mechanics at realistic aerodynamic Reynolds numbers will be paced by a broad range of fluid mechanical experiments. The experiments will include detailed probing of the mean and fluctuating flow-field quantities, closely

*Senior Staff Scientist.
†Research Scientist.
††Postdoctoral Research Associate.

spaced measurements of the surface skin friction, and determination of the positions of points of flow separation and reattachment, when these latter phenomena occur. It is these surface measurements that are the subject of this paper.

The methods available for measuring local skin friction at a surface include the following: (a) a momentum balance obtained from velocity and temperature profile measurements at two stations separated by a short distance; (b) extrapolation of mean velocity measurements very near the surface to provide an accurate velocity derivative at the wall; (c) a surface pitot tube; (d) hot-wire measurements of local turbulent shear stress extrapolated toward the wall; (e) a floating element of surface mounted on a balance; and (f) a heat-transfer surface element.

Method (a) is well suited to flows over flat plates; for flows with large pressure gradients along the surface, however, the inertia forces in the boundary layer so dominate the friction forces that small experimental errors in the velocity and temperature profiles cause large errors in the surface skin friction evaluated by this method. Methods (b) and (c) were shown by Bradshaw and Gregory (3) to contain inherent problems of calibration, even in flows with rather gentle pressure gradients. In particular, the methods showed inherent differences when used with laminar or turbulent boundary layers, and these differences would be aggravated in high Reynolds number tests with small scale models such as those usually used in fluid mechanics. The differences make methods (b) and (c) less general and, in addition, complicate the probe calibration process. These probes are usually calibrated in ducts, where the pressure gradients and the skin friction are intimately related through the effective duct diameter. Application of the probes to other conditions, e.g., adverse pressure gradients or very large Reynolds numbers, requires reliance on an assumed universal character of turbulent boundary layers well outside the viscous sublayers, a questionable procedure. Finally, intrusive probes generally are not suitable in fields of transonic flow or flows near separation because such flows are particularly sensitive to small disturbances. Crossed hot wires, which have been employed in method (d), are sufficiently long to encompass significant portions of a boundary-layer height at high Reynolds number. The measurements of shear stress are then not truly local in distance from the surface and contain significant errors caused by rapid changes in turbulence that occur over the length of the wire near a surface. Extrapolation of these data to the surface, especially in regions of pressure gradients where the total shear varies rapidly with distance from the surface (4), cannot be accurate.

Of the surface measurements, method (e), the floating element balance, measures the skin-friction force directly and is preferred whenever it can be employed. When small scale models are used, the size of the floating element, over which an average skin friction is measured, and the bulk of the instrument that must be contained within the model become serious drawbacks. The precision of their construction makes the balances so costly as to preclude the use of many elements even within large scale models, especially when consideration is given to their delicate nature and need for repeated repair. Finally, and perhaps most important, the floating element gage is sensitive to a surface pressure gradient that acts as a boundary force in the gap around the floating element and on the supporting beams within the gage in a manner indistinguishable from the skin-friction drag force. In some designs in which the gap widths vary with the load on the element, the error due to pressure gradients cannot even be estimated.

A skin-friction gage, utilizing the heat-transfer method - method (f) - that is free of some of these shortcomings was conceived originally by H. Ludwieg (5). The principle underlying this gage, illustrated in figure 1, requires the surface-heated element to have a dimension in the streamwise direction, Δx, that is small compared to the boundary-layer thickness. Then the heat transferred from the heated element, insulated from the surface material, forms a thermal boundary layer that lies within the viscous sublayer immediately adjacent to the surface. Here the transport processes are molecular and known, even when the boundary layer is turbulent and contains buffer and fully turbulent layers. Since the flow-field velocities which convect the heat in the viscous sublayer are predominantly proportional to the local wall shear, the rate of heat lost from the heated element becomes a measure of this wall shear (see, e.g., ref. 5). Surface pressure gradients also affect the velocity distribution here, but these effects are shown to be small in a properly designed gage.

The original Ludwieg gage was made of an electrically heated 2×9×6-mm block of copper. The 2×9-mm face was cemented to a circular disk of celluloid, 0.1 mm thick, that acted as a low thermally conductive support. The diaphragm was mounted flush with the surface of the model over a hole that housed the copper block and was oriented so that the 2-mm dimension was in the direction of the air flow. A vent equilibrated the pressure across the diaphragm. The gage was mounted in a flat plate model and was calibrated against boundary-layer surveys, method (a). The results possessed the character expected from Ludwieg's theoretical calculations, except the data were shifted in a manner to suggest significant conduction losses in the heater leads or thermocouple wires detecting the block temperatures. When calibrated, the gage was then used to measure the skin friction on the flat plate, but with nonzero pressure gradients imposed (6). It was assumed in reference 6 that the pressure gradients did not affect the gage calibration, and the consistency of the results tended to support this assumption. A drawback in using this gage in other applications is its size, not necessarily of the heater block, but of the supporting disk. Another drawback is the complexity of its design which is difficult to miniaturize. On models with pressure gradients, differential pressure loads on the thin supporting disk can also pose a problem.

Liepmann and Skinner (7) simplified the design of the gage while utilizing its basic idea. They merely buried a 12.7-μm-diameter platinum wire in a groove in the surface of an ebonite (bakelite) plate, with the axis of the wire mounted normal to the stream direction. The wire was heated electrically; the power supplied and the wire temperature were deduced from current and resistance measurements. The wire gage was calibrated with a hot-wire flow-field probe, method (b), on a flat plate model and, significantly, it was found that an identical calibration resulted when the flow in the boundary layer over the wire was either laminar or turbulent. One disadvantage, cited by the authors, was the effect of the direct thermal contact of the wire with its substrate. The conduction in the substrate appeared to have broadened the effective diameter of the wire to 5 mm from the actual wire diameter of 12.7 μm (see fig. 2). An ideal gage would produce a stepwise discontinuous surface temperature, whereas the Liepmann-Skinner gage apparently produced a long gradual temperature rise in the ebonite far ahead of the gage.

Later, the basic idea of the heated element gage was used by Bellhouse and Schultz in a series of experiments (see, e.g., refs. 8 and 9). The gage design they employed was a platinum film baked into the surface of a Pyrex glass substrate. Such a gage has the advantage of producing a rather smooth surface. Gages based on this design were made and tested on cylinders, the axes of which were normal to the stream, and on small movable probes that could be calibrated in channels and then mounted within specific models. One disquieting finding was the fact that the gage results differed when the boundary layer measured was laminar and when it was turbulent; this suggested more extensive conduction effects than even with the Liepmann-Skinner design.

The objective of the current investigation was to develop a gage design appropriate for use with a small-scale airfoil model in a high Reynolds number, transonic flow to investigate the mechanisms of shock-induced turbulent boundary-layer separation. The measurement of local skin friction at closely spaced stations is a key element of this investigation. At Reynolds numbers of 30×10^6, based on 30.48-cm chord length, most of the methods described previously would not apply. The possible methods were reduced to the heated-element skin-friction gage; the designs of either Liepmann and Skinner or Bellhouse and Schultz were favored because of their simplicity. We were concerned, however, about the apparent large conduction effect in the plastic substrate of the Liepmann and Skinner gage and about how this effect would be even larger on a glass substrate, assuming the Bellhouse-Schultz design was chosen. Liepmann and Skinner did not give the length of the wire they used in their gage so that their computation for Δx_{eff} could not be checked. The authors had reservations regarding the estimated magnitude of the conduction effect because it did not seem reasonable that conduction in a plastic substrate would alter the effective heated element width by a factor of 5 mm/12.7 μm or 400, and that if such a large effective width had resulted, that the laminar and turbulent boundary-layer data would have departed from each other. To clarify these points, a program was adopted to accomplish the following:

1. Construct a heated wire gage based on either the Liepmann-Skinner or Bellhouse-Schultz designs.
2. Determine if the gage can be reproduced through tight construction tolerances to avoid the need for calibrating each gage.
3. Test the gages in laminar and turbulent boundary layers.
4. Test the gage with pressure gradients.
5. Test a sequence of closely spaced gages to learn if the interaction between the gages can be used to detect the location of boundary-layer separation unambiguously.

HEATED-ELEMENT SKIN-FRICTION GAGE DESIGN CRITERIA

An early design consideration for a heated wire or film gage is the choice of the substrate material acting as the wire or film support. To keep the effective streamwise dimension short, the material should possess the lowest possible thermal conductivity so that the surface temperature in the vicinity of the heated element approaches the ideal (see fig. 2). Pyrex glass, used by Bellhouse and Schultz, has a conductivity of about 0.011 W/cm² (°C/cm), whereas the ebonite used by Liepmann and Skinner has a value of approximately 0.0078 W/cm² (°C/cm). The material used here was styrene copolymer with a conductivity of k = 0.0015 W/cm² (°C/cm). One difficulty with the use of low-conductivity plastic, however, is its low melting temperature which eliminates the possibility of building the gage by painting the surface element with a platinum salt and firing it into a metallic film, as was done by Bellhouse and Schultz. The authors tried to vapor plate or to sputter metallic films onto the plastic substrate, but met with little success when the streamwise dimension across the film was kept to the order of 0.2 mm or less. Despite considerable care in plating these films, a large fraction contained, or soon developed, open circuits when the films were this narrow. To avoid these difficulties and still retain a narrow gage, the Liepmann-Skinner approach was adopted, but with platinum-rhodium wire, 0.0025 cm in diameter, as the heater element.

A second design consideration was the allowable waviness or surface "roughness" that could be introduced by the heater element. Burying the wire in a groove was found to be difficult because the milled grooves, nominally 0.0025 cm deep, proved to have varying depths, up to a factor of 2, so that there was no assurance that any one wire was buried to the same depth along its length or that different wires were exactly at the same depth. It was decided to lay the wires on top of the plastic surface between two previously mounted leads that came up from the inside of the plastic. A thin layer of epoxy (< 25 μm) was cast between adjacent wires, and the entire surface was handworked to yield a surface such as that indicated in the sketch in figure 3. The allowable waviness, indicated in the sketch with an h, was established by requiring that

$$h \frac{\sqrt{\tau_w \rho_w}}{\mu_w} < 5 \qquad (1)$$

i.e., keeping h less than the viscous sublayer thickness. For example, at a Reynolds number of 16×10^6 on a model 7.5 cm from the leading edge, the value of h satisfying eq. (1) is 3.5×10^{-3} mm. The waviness of surfaces actually fabricated was found to be 2×10^{-3} mm over two representative samples.

Liepmann and Skinner developed the conditions that the dimension of the heater element should satisfy:

$$1 << Nu < \frac{Pr}{c_f} \qquad (2)$$

The lower limit ensures that the element is sufficiently large so that boundary-layer theory can be applied over the surface of the element with an ideal stepwise discontinuous surface temperature distribution (see fig. 2). This condition offers little constraint even for dimensions as small as $\Delta x = 25$ μm at the high Reynolds numbers of turbulent boundary layers. The upper limit is set by the requirement that the gage behave the same in a laminar or turbulent boundary layer. This limit can be re-expressed in a more precise form utilizing the detailed thermal analysis of Spalding (10 and 11), as shown in the appendix. A turbulent boundary layer yields skin-friction results within 10% of the results of a laminar boundary layer if

$$\frac{\sqrt{\tau_w \rho_w}}{\mu_w} \Delta x < 435 \qquad (3)$$

for air with a Prandtl number of 0.7. This condition is comparable to the Liepmann-Skinner condition of eq. (2), and limits the power dissipation from the heated element to

$$\frac{i^2 R}{W \Delta T} < 1.1 \text{ W/m °C} \qquad (4)$$

in air.

One other factor requiring consideration is the effect of pressure gradient along the surface on the instrument's readings. Liepmann and Skinner first analyzed this effect near a point of separation where $\tau_w \to 0$. Later Bellhouse and Schultz extended these calculations to account for the local shear as well. Their result can be rewritten in the form

$$\frac{\tau_w}{(\tau_w)_{FP}} = 1 + \frac{0.02}{Nu} \frac{1}{(c_f/2)_{FP}} \frac{\Delta x}{u_e} \frac{du_e}{dx} \qquad (5)$$

For turbulent boundary layers, $Nu \approx 10$ and $(c_f/2)_{FP} \approx 0.001$, which makes the factor ahead of $\Delta x/u_e(du_e/dx)$ in eq. (5) equal to about 2. For example, if $u = cx$, as on a blunt forebody, the term accounting for the boundary-layer acceleration is equal to $2(\Delta x/x)$. Thus, gages with effective widths, Δx, that are small compared to the length of run, can be expected to be relatively insensitive to boundary-layer accelerations. This requirement further supports the need for a low conductivity substrate.

CALIBRATION OF THE GAGE IN A TURBULENT BOUNDARY LAYER

A plug containing four gages, constructed as indicated in figure 3, was made to test the reproducibility of the construction technique, to provide a multiple set of calibration specimens, and to permit investigating the interaction between wire gages that are closely spaced. The distance between the gages in the flow direction is 0.32 cm in the test plug. The plug was mounted as shown in figure 4 in the wall of a wind tunnel alongside a floating element gage, used as a calibration standard. The floating element gage was calibrated by attaching known weights to the balance element; because the pressure was uniform on the tunnel wall in the region of the balances, accurate readings of the shear forces were expected from this instrument. It should be noted that the floating element has a diameter of 0.94 cm, and the contrast in streamwise distance covered by the floating element and individual wire gages is dramatic. A standard constant-temperature hot-wire power supply and output amplifier was attached to the wire gages. It was found that overheat temperatures of at least 20°C were needed to make the heat lost from a wire proportional to its temperature rise, or $i^2R/\Delta T$ a constant. The wind tunnel was operated at stagnation pressures that produce Reynolds numbers of 50×10^6/m; the Mach number of the stream was maintained at approximately 0.7. The boundary layer on the wind-tunnel wall was fully turbulent.

In the first series of tests, only one of the four wires was heated at a time. The results of the calibration of a single wire are shown in figure 5. The ordinate is the power dissipated within the wire per unit temperature rise. The abscissa is the cube root of the product of the local wall shear and the air density evaluated at the surface temperature upstream of the wire. These coordinates are used because the theoretical formulations (10) of an ideal gage performance (stepwise surface temperature discontinuity, laminar transfer mechanisms) indicate that a straight line should result. The choice of wall properties, ρ_w, was suggested originally by Liepmann and Skinner from analysis, and demonstrated by Bellhouse and Schultz to hold under a range of Mach numbers. To a first order, the data lie on the straight line as would be expected since the criterion expressed by eq. (4) is satisfied. The calibrations of the other wires on the plug agreed within ±2% with the results shown, indicating good reproducibility in the construction technique.

A test with the four-element plug was made to determine the interference between adjacent plugs. This was accomplished by heating two elements to a specified temperature simultaneously, and then noting the change in power required to maintain the same temperature in one of the wires when the other was turned off. The results showed that it was the downstream wire that was affected through the interference, indicating that it is the heat carried by the airstream, rather than conduction in the substrate, that produces the interference. This observation is consistent with the small Δx_{eff} noted later. When the wires were 3.2 mm apart, the

heat from the upstream wire reduced the power lost from the downstream wire by 4%, a value that would be represented as a 12% error in shear by the wire calibration. When the wires were twice as far or 6.4 mm apart, the corresponding error in the shear measurement of the downstream wire would be 4.2%. At a separation distance of 9.6 mm the shear error in the downstream wire measurement is reduced to 3%. For skin-friction tests at shear stresses within the calibration range then, spacings of about 1 cm between successively heated wires are needed to eliminate interference of the upstream gages on those downstream in a model with a series of skin-friction gages. The interference effect, however, can be exploited in a flow separation detector described later.

To compare the different styles of gages, figure 6 shows the current calibration results and those of Ludwieg and of Bellhouse and Schultz. The Liepmann-Skinner gage calibration is not shown because the gage length across the flow, W, was not specified in their report and thus their data could not be replotted. It would be expected, however, that the Liepmann-Skinner results would be between the present results and those of Bellhouse and Schultz. In this figure, the ordinate is divided by the gage width, W, in order to make the slopes of the lines depend only on the effective length of the gage in the streamwise direction. In this coordinate system, the intercept is a measure of the quantity of heat conducted into the substrate; a larger slope means a larger effective length of the gage in the streamwise direction (slope $\propto (\Delta x_{eff})^{2/3}$). As expected from the design criteria discussion in the previous section, the Bellhouse-Schultz gage utilizing the Pyrex substrate shows the highest heat conduction effects by having the largest intercept and the greatest slope. The present gage has significantly lower heat-conduction losses and the $(\Delta x)_{eff}$ found from the slope of the calibration line turns out to be 6×10^{-2} mm, or only about 2.5 times the wire diameter. This finding is so different from the one quoted by Liepmann and Skinner ($\Delta x_{eff}/\Delta x = 390$) that their results are inexplicable, even when consideration is given to the differences in the substrate thermal conductivities. The Ludwieg gage results fall between the present results and those of Bellhouse and Schultz, again as expected from the design of the gage. It is noted that the Bellhouse-Schultz gage violates the criterion represented by eq. (4) and, indeed, the authors report somewhat different calibrations in laminar and turbulent boundary layers in their work.

SKIN FRICTION IN THE LAMINAR BOUNDARY LAYER OF A CYLINDER

Because the calibration of the heated-element skin-friction gage indicated a very small Δx_{eff}, it would be expected that this gage would be suitable for use on very small models and where pressure gradients exist along the surface - see eq. (5). Also, the gage satisfies condition (4) so that it would also be expected to perform the same with either laminar or turbulent flow.

In using a gage on a wind-tunnel model, calibration of the particular gage employed is generally required. Bellhouse and Schultz alluded the technique of building a movable gage that could be calibrated one place and then moved bodily and installed into a model. The present design is also suitable for such an approach. The authors, however, were interested in learning if careful control of the construction of the gage could obviate the need for calibrating each gage. To test this idea, but to avoid building many gages, a model was chosen that can yield well-resolved, skin-friction information with a single gage; namely, a circular cylinder with its axis placed normal to an airstream and able to rotate about this axis. A single static pressure tap was also placed in the model. The test cylinder is 19 mm in diameter and made of stainless steel. The gage was made on a stainless insert to close tolerances relative to the calibrated gages. For example, the cold resistance of the gage is 2.61 Ω, which is within 2% of the cold resistance of the calibrated gages. The gage, mounted in place, is shown on the cylinder in figure 7 and in greater detail in figure 8.

The test with the cylinder was run in a small, low-speed wind tunnel at $M = 0.3$. The air is drawn into the wind tunnel from the laboratory room so that the stagnation pressure is 1 atm and the temperature is 21°C. The Reynolds number thus achieved on the cylinder, based on diameter, is 1.2×10^5 which places test conditions in the subcritical range prior to the onset of turbulent flow. The pressure distribution around the cylinder is shown in figure 9. The pressure drops with angular position from the stagnation point to a minimum at about 68°, recovers some to about 82°, and then levels off. The shape of the pressure distribution suggests that the boundary layer has separated just ahead of the 80° position.

The corresponding skin-friction measurements are shown on figure 10. The circled data points represent the heated gage skin-friction measurements based on the calibrations made in the turbulent boundary on the wind-tunnel wall (fig. 5). The solid line represents the skin friction calculated with a finite difference boundary-layer program utilizing laminar transport properties (12) and incorporating the pressure distribution of figure 9. The agreement of the laminar boundary-layer results with the measurements, based on a previous calibration of similar gages, is remarkably good up to an angle of $\theta = 50°$ from the stagnation point. Beyond this point, the measured points show a progressively increasing departure from the laminar boundary-layer theory; at 60° and 70° the data are 11 and 72% lower than the theoretical results, respectively. Since the principal departure occurs at $\theta = 70°$, which is a point where the local pressure gradient is not large (it is near a minimum in the pressure distribution), the cause for the behavior noted is not understood. The agreement noted at $\theta = 10°$, where the level of shear is about the same as at $\theta = 70°$, excludes a basic calibration error.

SEPARATION DETECTOR

An adaptation of the skin-friction gage was used as a flow direction indicator to identify

positions of separated flow. In references 13 and 14, Kooi and Vidal et al. point out that separated flow fields (local flow reversals) often accompany the interaction of a normal shock wave with a turbulent boundary layer, and that these regions can be very thin and difficult to define using present techniques (pitot tubes, oil flows, orifice dams, etc.). Bellhouse and Schultz (9) used the presence of an irregular response of a single heated element as an indication of separation in laminar flow. This technique, however, can be confused by the presence of periodic transition to turbulence. For fully turbulent flows, careful harmonic analysis of the dynamic signals from the gages could possibly distinguish the presence of separation. A completely unambiguous and much simpler approach, however, is to exploit the interaction of multiple heated element gages when they are close together.

The experiment was conducted in the NASA-Ames Research Center's High Reynolds Number Facility with the test section and flow conditions as indicated in figure 11a. Wall static pressure taps were spaced on a line at 25.4 mm intervals in the upstream portion of the test section and 50.8 mm intervals downstream. The separation detector ports were located on a line at seven positions along the tube and at 45° around the tube from the line of static pressure taps. To produce the separation, a normal shock wave could be positioned at any station inside the test section by means of a hollow, cylindrical, shock-wave generator that was inserted into the exit. The separation detector was constructed in a manner similar to the skin-friction gages, but on a surface with transverse curvature to fit the wall of the circular test section. Details of the separation detector plug configuration are shown in figure 11b. The manner of operation of this detector was to heat the center detector wire to rather high temperature. The adjacent sensor wires were maintained at low overheat temperatures, just high enough to permit power loss measurements. In this mode of operation, the sensor wire locally downstream of the heated detector wire requires the lesser power for a specified overheat temperature.

The results of this investigation are presented in figures 11 and 12. Figure 11 illustrates the response of the gage to passage of the shock wave. The abscissa represents the position of the detector relative to the shock wave, with negative values indicating that the detector is upstream of the shock wave. The upper curve is the wall static pressure of the detector location, and the remaining curves are the bridge voltages to the upstream and downstream (relative to the main stream) sensor wires and their difference. The local flow reversal associated with the passage of the shock wave over the detector is dramatically illustrated by the opposite response of the upstream and downstream wires. As the shock wave passes, the temperature of the flow surrounding the wires decreases on the downstream and increases on the upstream side of the heater. This indicates that heated fluid is locally being transported toward the upstream sensor wire. The difference curve amplifies these effects and can be used to define both the separation (S = 0) and reattachment (R = 57.2 cm) points.

The effect of Reynolds number on the length of separated flow is shown on figure 13. Here the length of separation, S_p, is normalized by the undisturbed boundary-layer thickness, δ_u, just upstream of the interaction, and is plotted as a function of Reynolds number based on δ_u. Also, a comparison is made with previous investigations (refs. 13 through 15) for normal shock wave, turbulent boundary-layer interactions where pitot tubes were utilized. The paucity of data makes it very difficult to establish trends from the previous results. The present data which were obtained over essentially the same Mach and Reynolds number range indicate that the length of the separated flow field scales directly with the boundary-layer thickness ahead of the interaction. Also the length of separated flow is much larger when measured by the present technique. Clearly, additional data are needed over a wider Reynolds number range to corroborate the trends found of the present investigation; however, it does appear that intrusive pitot probes or thick oil films used by the other investigators may seriously disturb these types of flow fields.

CONCLUDING REMARKS

The study described has demonstrated the usefulness of an individual heated-film gage in measuring skin friction and, in closely spaced groups, in measuring the location of separation and reattachment without disturbing the flow. It was shown that a key element in making the skin-friction gage universally applicable, i.e., independent of laminar or turbulent flow and insensitive to pressure gradients, is the use of a very low thermal conductivity mount or substrate to support a fine heated film or wire. For separation detection, the use of multiple elements eliminates the need for complex fluctuating signal processing and permits unambiguous interpretation of the results. The manner in building these gages, of laying wires onto the substrate, filling between with plastic, and handworking the surface is admittedly complex, but was manageable because of the fine manual skills of the authors' technician, Mr. Fred Lemos, as is evidenced by the reproducibility of the gages. The styrene substrate proved to be incompatible with vapor plating or sputtering films less than 0.03 mm wide at thicknesses of less than 10^{-4} mm, at least with the laboratory techniques and limited effort used by the authors and some fairly experienced technicians. Plating has distinct advantages of achieving smooth surfaces ($h < 10^{-4}$ mm) and uniformity of construction and this work is not intended to discourage that approach. In fact, the authors themselves have initiated contacts with the microelectronics industry to see if the skills developed there in plating circuits can be exploited in the production of these gages.

REFERENCES

(1) D. R. Chapman, H. Mark, and M. W. Pirtle, "Computers vs. Wind Tunnels for Aerodynamic Flow Simulation," ASTRONAUT. AND AERONAUT., VOL. 13, pp. 22-30; April 1975.

(2) B. E. Launder and D. B. Spalding, "Mathematical Models of Turbulence," Academic Press; 1972.

(3) P. Bradshaw and N. Gregory, "The Determination of Local Turbulent Skin Friction from Observations in the Viscous Sublayer," AERO. RES. COUNC., London, Reports and Memoranda No. 3202; March 1959.
(4) Chen-Chi Sun and M. E. Childs, "Calculation of Turbulent Shear Stress in Supersonic Boundary Layer Flows," AIAA TN, VOL. 13, No. 2, pp. 224-226; Feb. 1975.
(5) H. Ludwieg, "Instrument for Measuring the Wall Shearing Stress of Turbulent Boundary Layers," NACA TM 1284; 1950.
(6) H. Ludwieg and W. Tillman, "Investigations of the Wall-Shearing Stress in Turbulent Boundary Layers," NACA TM 1285; May 1950.
(7) H. W. Liepmann and G. T. Skinner, "Shearing-Stress Measurements by Use of a Heated Element," NACA TN 3268; 1954.
(8) B. J. Bellhouse and D. L. Schultz, "The Measurement of Skin Friction in Supersonic Flow by Means of Heated Thin Film Gages," AERONAUT. RES. COUNC., Reports and Memoranda No. 3490; Oct. 1965.
(9) B. J. Bellhouse and D. L. Schultz, "Determination of Mean and Dynamic Skin Friction, Separation, and Transition in Low-Speed Flow with a Thin Film Heated Element," J. FLUID MECH., VOL. 24, part 2, pp. 379-400; 1966.
(10) D. B. Spalding, "Heat Transfer to a Turbulent Stream from a Surface with a Stepwise Discontinuity in Wall Temperature," International Developments in Heat Transfer, PROC. ASME Conference, Boulder, Colo., part II, pp. 439-446; 1961.
(11) D. B. Spalding, "Contribution to the Theory of Heat Transfer Across a Turbulent Boundary Layer," INT. J. HEAT MASS TRANSFER, VOL. 7, pp. 743-761; 1964.
(12) J. G. Marvin and Y. S. Sheaffer, "A Method for Solving the Nonsimilar Laminar Boundary-Layer Equations Including Foreign Gas Injection," NASA TN D-5516; Nov. 1969.
(13) J. W. Kooi, "Experiment on Transonic Shock-Wave Boundary-Layer Interaction. AGARD Conference on Flow Separation," AGARD-CPP-168, Paper No. 30; 1975.
(14) R. J. Vidal et al., "Reynolds Number Effects on the Shock Wave - Turbulent Boundary Layer Interaction at Transonic Speeds," AIAA Paper No. 73-661; July 1973.
(15) J. Seddon, "The Flow Produced by Interaction of a Turbulent Boundary Layer with a Normal Shock Wave of Strength Sufficient to Cause Separation," ARC R and M No. 3502; March 1960.

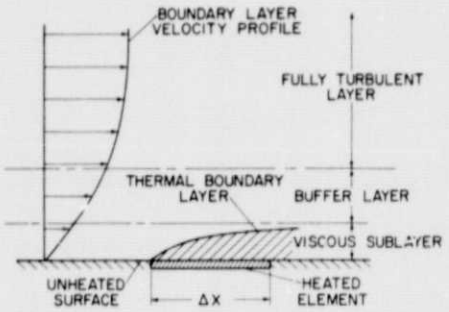

Fig. 1. Principle of heated film skin-friction gage.

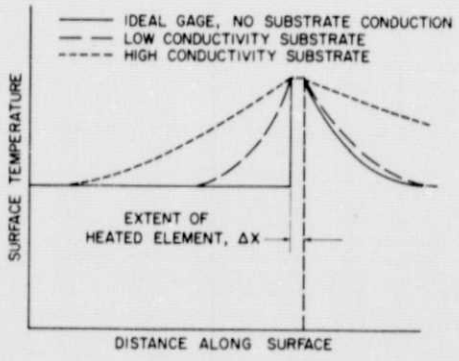

Fig. 2. Effect of heat conduction on the surface temperature in the vicinity of the heated element.

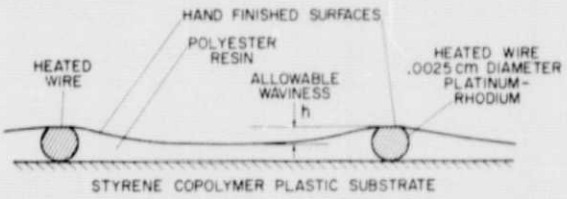

Fig. 3. Construction details of heated wire skin-friction gage.

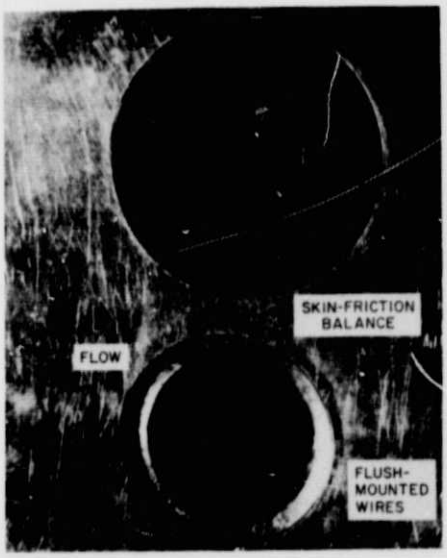

Fig. 4. Calibration arrangement on wind-tunnel wall.

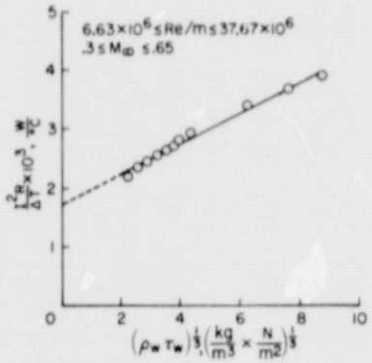

Fig. 5. Calibration of heated wire skin-friction gage.

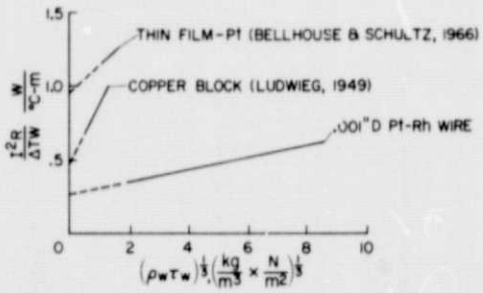

Fig. 6. Comparison of the performance of various heated film gages.

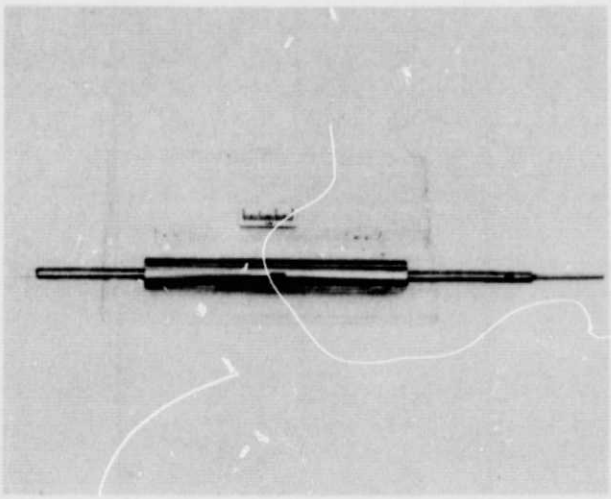

Fig. 7. Cylindrical wind-tunnel model.

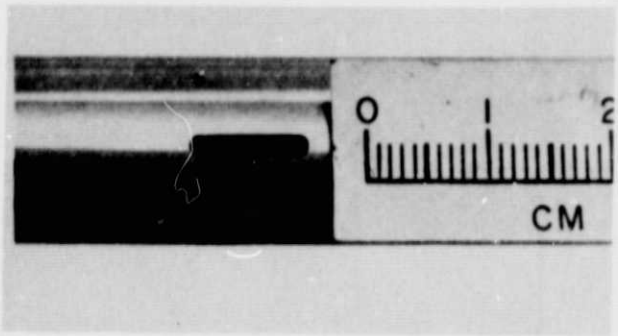

Fig. 8. Detail of heated wire skin-friction gage in cylindrical model.

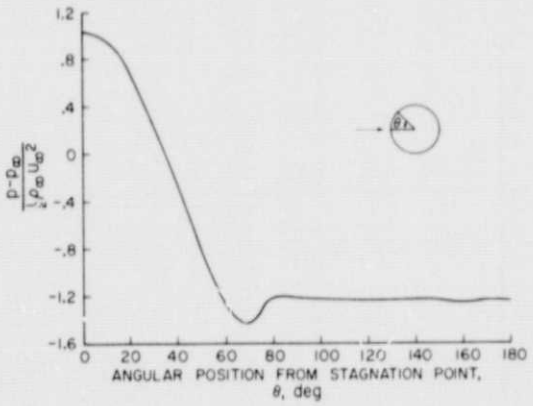

Fig. 9. Pressure coefficient distribution around cylindrical model in cross flow; Diam. = 19.05 mm, $Re_D = 1.2\times10^5$, $M_\infty = 0.3$.

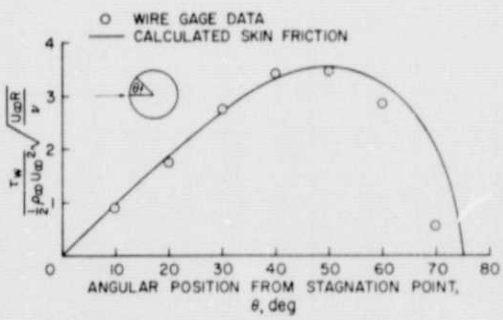

Fig. 10. Skin-friction distribution around periphery of cylindrical model; Diam. = 19.05 mm, $Re_D = 1.2\times10^5$, $M_\infty = 0.3$.

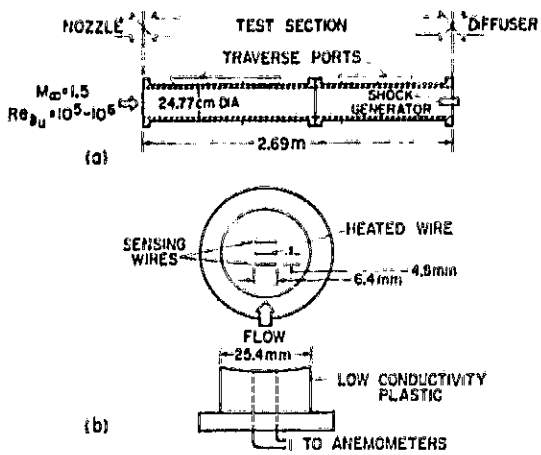

Fig. 11. Test section and detector used in separation experiment; (a) test section, (b) separation detector.

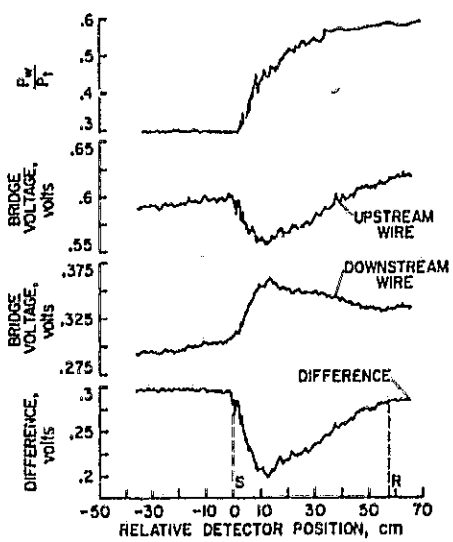

Fig. 12. Response of separation detector to shock-wave traverse.

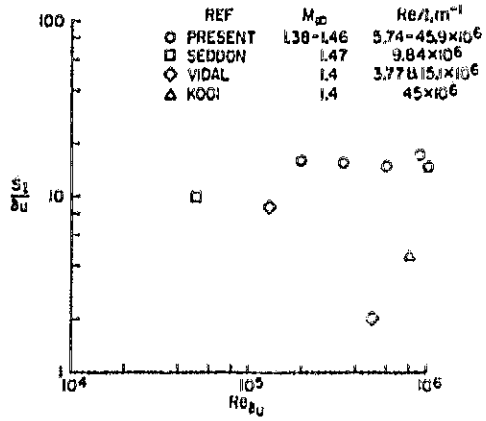

Fig. 13. Effect of Reynolds number on the length of separated flow.

APPENDIX

Upper Limit of Gage Dimension in Streamwise Direction

If the extent of the gage in the streamwise direction is sufficiently small, it behaves the same in either a laminar or turbulent boundary layer. The limit of this extent can be evaluated from Spalding's theory (refs. 10 and 11) for the heat transfer into a turbulent boundary layer downstream of a surface temperature jump. Near the stepwise discontinuous surface temperature, the local Stanton number and skin-friction coefficient can be related by the series

$$\frac{x^+}{Pr} = 0.157\,\delta^3 + 9.41\times10^{-7}\,\delta^7 + \ldots \qquad (A1)$$

where

$$x^+ = \int_{\ell}^{x} \frac{u_e\sqrt{c_f/2}}{\nu_w}\,dx' \qquad (A2)$$

$$\delta = \frac{\sqrt{c_f/2}}{St} \qquad (A3)$$

ℓ = station where surface temperature jump occurs

Pr = Prandtl number of fluid

St = local Stanton number

c_f = local skin friction coefficient

u_e = local velocity at boundary-layer edge

x = station downstream of temperature jump

ν_w = local kinematic viscosity based on surface temperature

The first term in the series results from heat exchange totally within the laminar sublayer and agrees with the result corresponding to a fully laminar boundary layer. The second and subsequent terms introduce the effects of turbulence in the buffer region and outer parts of the turbulent boundary layer. We now seek the value of $\Delta x = \ell - x$ where the turbulent contributions are small. To do this it is first necessary to evaluate the *average* Stanton number over the entire gage, where

$$\overline{St} = \frac{1}{\Delta x}\int_0^{\Delta x} (St)\,dx' \qquad (A4)$$

In terms of δ in eq. (A3), the mean Stanton number is

$$\overline{St} = \frac{1}{x^+}\int_0^{x^+} \frac{\sqrt{c_f/2}}{\delta}\,dx^+ = \frac{\sqrt{c_f/2}}{x^+}\int_0^{x^+} \frac{dx^+}{\delta} \qquad (A5)$$

when x^+ is small and the mean value theorem is invoked with c_f evaluated between ℓ and x, with $\Delta x \ll \ell$. From eq. (A1)

$$dx^+ = Pr\{0.47\,\delta^2 + 6.59\times10^{-6}\,\delta^6 + \ldots\}d\delta \qquad (A6)$$

With eq. (A6) substituted into eq. (A5), the average Stanton number over the gage is found directly to be

$$\overline{St} = \frac{\sqrt{c_f/2}}{x^+}\,(0.165\,\delta^2 + 7.68\times10^{-7}\,\delta^6 + \ldots) \qquad (A7)$$

for $Pr = 0.7$. From eq. (A1) and $Pr = 0.7$

$$x^+ = 0.11\,\delta^3 + 6.59\times10^{-7}\,\delta^7 + \ldots \qquad (A8)$$

From eqs. (A7) and (A8), the value of x^+ where the value of $\overline{St}$ is 3.2% larger than for a laminar boundary layer is

$$x^+ = \frac{u_e\sqrt{c_f/2}\,\Delta x}{\nu_w} = \frac{\sqrt{\tau_w\rho_w}\,\Delta x}{\mu_w} = 435.6$$

Since $\tau \sim \overline{St}^3$, at this value of x^+, or less, the gage will give skin-friction results within 10% for a given $\overline{St}$ if the boundary layer is either laminar or turbulent.